Phase diagrams of a model for two-layer ^{3}He-^{4}He mixture films

K. K. Mon* and W. F. Saam
Department of Physics, The Ohio State University, Columbus, Ohio 43210
(Received 15 September 1980)

We present a Migdal-Kadanoff renormalization-group scheme for a model two-layer classical XY system with annealed impurities. The model Hamiltonian is appropriate for a two-layer ^{3}He-^{4}He mixture system. We find a rich variety of phase diagrams. Depending on the choice of parameters we find either one or two first-order phase-separation transitions, which may be accompanied by the appearance of superfluidity. Phase diagrams with two λ lines are found, making possible two distinct transitions in the superfluid density. In the case of phase-separation transitions, each transition is primarily associated with a single layer, and three-phase coexistence is possible. Comparison with recent experiments is made.

I. INTRODUCTION

In this work we treat a two-layer generalization of a single-layer model introduced by Berker and Nelson[1] and Cardy and Scalapino[2] (hereafter referred to as BNCS) for the description of ^{3}He-^{4}He mixture films. Our primary motivation for this work is to explore the consequences of departing from a purely two-dimensional framework. Indeed, we find that the additional degrees of freedom in the two-layer model, when the effect of a substrate potential are included, produce phase diagrams possessing considerably more complexity than do those of the one-layer model.

The model Hamiltonian to be used is set on two parallel triangular lattices positioned such that each site on the lower lattice lies directly above its counterpart on the upper lattice. Each lattice site may be occupied by either a ^{4}He atom or a ^{3}He atom. Nearest-neighbor sites occupied by ^{4}He atoms interact via XY couplings, and all nearest-neighbor pairs possess Ising lattice-gas couplings. Differing chemical potentials for the layers introduce the effect of a substrate potential. Explicitly, we write

$$
\begin{aligned}
H = {} & \frac{J_1}{2}\sum_{\langle ij\rangle}|\nu_i^{(1)}e^{i\theta_i^{(1)}}-\nu_j^{(1)}e^{i\theta_i^{(2)}}|^2+\frac{J_2}{2}\sum_{\langle ij\rangle}|\nu_i^{(2)}e^{i\theta_i^{(2)}}-\nu_j^{(2)}e^{i\theta_j^{(2)}}|^2+\frac{J_x}{2}\sum_i|\nu_i^{(1)}e^{i\theta_i^{(1)}}-\nu_i^{(2)}e^{i\theta_i^{(2)}}|^2 \\
& +\sum_{\langle ij\rangle}[K_{44}^{(1)}\nu_i^{(1)}\nu_j^{(1)}+K_{34}^{(1)}\nu_i^{(1)}(1-\nu_j^{(1)})+K_{34}^{(1)}\nu_j^{(1)}(1-\nu_i^{(1)})+K_{33}^{(1)}(1-\nu_i^{(1)})(1-\nu_j^{(1)})+K_{44}^{(2)}\nu_i^{(2)}\nu_j^{(2)} \\
& \quad +K_{34}^{(2)}\nu_i^{(2)}(1-\nu_j^{(2)})+K_{33}^{(2)}(1-\nu_i^{(2)})(1-\nu_j^{(2)})+K_{34}^{(2)}\nu_j^{(2)}(1-\nu_i^{(2)})] \\
& +\sum_i[K_{44}^{x}\nu_i^{(1)}\nu_j^{(2)}+K_{34}^{x}\nu_i^{(1)}(1-\nu_i^{(2)})+K_{33}^{x}(1-\nu_i^{(1)})(1-\nu_i^{(2)})+K_{34}^{x}\nu_i^{(2)}(1-\nu_i^{(1)})] \\
& -\sum_i[\mu_3^{(1)}(1-\nu_i^{(1)})+\mu_3^{(2)}(1-\nu_i^{(2)})+\mu_4^{(1)}\nu_i^{(1)}+\mu_4^{(2)}\nu_i^{(2)}] \ . \qquad (1)
\end{aligned}
$$

Here $\sum_{\langle ij\rangle}$ means a sum over distinct nearest-neighbor pairs on a triangular lattice, while $\sum_i$ indicates a sum over sites on that lattice. J_1 and J_2 are intralayer XY couplings, while J_x is the analogous interlayer coupling. $K_{\alpha\gamma}^{(\beta)}$ is the interaction energy of nearest neighbors of types α and γ ($\alpha,\gamma=3,4$) on lattice β ($\beta=1,2$). $K_{\alpha\gamma}^{x}$ is interlayer coupling for atoms of types α and γ. $\mu_\alpha^{(\beta)}$ is the chemical potential of a particle of type α on lattice β. The variable $\nu_i^{(\beta)}$ takes on two values, zero when site i on lattice β is occupied by a ^{3}He atom and unity when the site is occupied by a ^{4}He atom. Finally, $\theta_i^{(\beta)}$ is the phase of a ^{4}He atom on site i of lattice β.

Within an irrelevant constant term, H may be writ-

ten in the more compact and useful form

$$H = J_1 \sum_{\langle ij \rangle} \nu_i^{(1)} \nu_j^{(1)} V_{xy}(\theta_i^{(1)} - \theta_j^{(1)}) + J_2 \sum_{\langle ij \rangle} \nu_i^{(2)} \nu_j^{(2)} V_{xy}(\theta_i^{(2)} - \theta_j^{(2)}) + J_x \sum_i \nu_i^{(1)} \nu_i^{(2)} V_{xy}(\theta_i^{(1)} - \theta_i^{(2)})$$
$$+ K_1 \sum_{\langle ij \rangle} (\nu_i^{(1)} - \nu_j^{(1)})^2 + K_2 \sum_{\langle ij \rangle} (\nu_i^{(2)} - \nu_j^{(2)})^2 + K_x \sum_i (\nu_i^{(1)} - \nu_i^{(2)})^2 - \mu_1 \sum_i \nu_i^{(1)} - \mu_2 \sum_i \nu_i^{(2)} \ , \quad (2)$$

in which

$$K_1 = \tfrac{1}{2}(J_1 - K_{44}^{(1)} - K_{33}^{(1)} + 2K_{34}^{(1)}) \ ,$$
$$K_2 = \tfrac{1}{2}(J_2 - K_{44}^{(2)} - K_{33}^{(2)} + 2K_{34}^{(2)}) \ ,$$
$$K_x = \tfrac{1}{2}(J_x - K_{44}^{x} - K_{33}^{x} + 2K_{34}^{x}) \ , \quad (3)$$
$$\mu_1 = \mu_4^{(1)} - \mu_3^{(1)} + 3(K_{33}^{(1)} - K_{44}^{(1)}) + \tfrac{1}{2}(K_{33}^{x} - K_{44}^{x}) \ ,$$
$$\mu_2 = \mu_4^{(2)} - \mu_3^{(2)} + 3(K_{33}^{(2)} - K_{44}^{(2)}) + \tfrac{1}{2}(K_{33}^{x} - K_{44}^{x}) \ ,$$
$$V_{xy}(\theta) = 1 - \cos\theta \ .$$

At this point it is useful to elaborate on the effect of a substrate potential. Since ^{3}He and ^{4}He atoms are isotopes, the potential couples to them equally. However, quantum effects are quite important in the helium mixtures. For example, near a wall bounding a bulk mixture a strong concentration gradient is produced because the smaller zero-point motion induced volume of the ^{4}He atom makes it energetically favorable to have an excess of ^{4}He atoms located in the attractive well of the wall potential.[3] Further, at the free surface of a bulk mixture there is a bound state of a ^{3}He atom due primarily to the relatively large zero-point motion of this atom.[4] In a thin film the quantum effects are perhaps even more interesting. The free surface state for a ^{3}He atom appears to remain, but the bulk states become discrete due to the presence of the substrate just below the surface. In very thin films recent work of DiPirro and Gasparini[5] shows that in some cases only two important states remain, one localized within the ^{4}He and the other near the surface. Though we cannot explicitly put quantum effects in our inherently classical calculations we can model the two-quantum-state effect by including in μ_1 and μ_2 one-body terms which are different for ^{3}He's in each layer. This allows us to consider nonzero values of the difference $\Delta\mu = \mu_2 - \mu_1$ even in the situation where the Ising couplings are the same in each layer. The naive omission of quantum effects would yield $\Delta\mu = 0$ in the case of equal Ising couplings since explicit substrate potential terms would cancel in $\Delta\mu$, the helium atoms being isotopes.

It is possible to provide order-of-magnitude estimates of the parameters appearing in Eq. (3) for the ^{3}He-^{4}He mixture system. Based on bulk properties, we expect that

$$K_{44}^{(\beta)} + K_{33}^{(\beta)} - 2K_{34}^{(\beta)} \sim n_4[(\partial\mu_4/\partial n_4)_{n_3 T} + (\partial\mu_3/\partial n_3)_{n_4 T} - 2(\partial\mu_4/\partial n_3)]_{n_4 T} \ ,$$

where μ_3 and μ_4 are the bulk ^{3}He and ^{4}He chemical potentials, n_3 and n_4 are the corresponding number densities, and $\beta = 1, 2, x$. The dilute-solution theory of Baym[6] says that the term in brackets here is zero at low temperatures; thus, we at least expect it to be small compared to $n_4(\partial\mu_4/\partial n_4)_{n_3 T} \sim 27 k_B$. The parameters J_1, J_2, and J_x are of order $n_4\hbar^2 a k_B/m \sim k_B$, where m is the ^{4}He atomic mass, and a is an interatomic spacing. Assuming that the Ising couplings are approximately independent of layer index β, we expect $\Delta\mu \equiv \mu_2 - \mu_1$ to be of the order of the level difference found by DiPirro and Gasparini.[5] This gives $\Delta\mu \sim k_B$.

The discrete ^{3}He level nature of thin mixture films makes somewhat plausible our two-layer lattice model which might at first glance appear to not represent very well a continuum film system. Many of our most interesting results are primarily a consequence of having two discrete layers. In particular, we find that, for a range of coupling parameters, our system can undergo two superfluid transitions, a phenomenon which has been observed in very recent experiments of Bishop and Reppy,[7] and which cannot be explained by the BNCS theory.

To exhibit these novel features, we have chosen a particular set of coupling parameters (in units of Boltzmann's constant $k_B = 1$) $J_1 = J_2 = K_1 = K_2 = K_x = 1.0$ and $J_x = 0.05$ for which we determine the phase diagrams over a wide range of temperature and chemical potential using a generalized Migdal-Kadanoff renormalization-group method. The rather small interlayer XY coupling ($J_x = 0.05$) was chosen for reasons of computational efficiency as the numerical method requires lengthy calculation; recent study[8] of a pure ^{4}He system indicate that no qualitative changes occur for $J_x \sim 1$. There is further discussion of this point in Sec. V.

In the next section, we will consider a Migdal-Kadanoff[8–10] renormalization-group transformation to be used in affecting approximate determinations of the phase diagrams produced by H. We also derive an approximate expression for the superfluid areal

density $\sigma_s(T)$ for our two-layer system. In Sec. III we describe the phase diagrams which we have obtained. Some discussion is also given concerning the consequences of varying the Ising and XY couplings. In Sec. IV we describe in detail how the phase diagrams were found. Section V contains a comparison of our results with available experimental data and some additional remarks.

II. RENORMALIZATION-GROUP METHODS

The Hamiltonian in the form (2) is not invariant under the Migdal-Kadanoff renormalization-group transformation to be introduced shortly. It is more appropriate to redefine H in terms of a sum of general *four-site* interactions $h_{4ij}^{(n)}(\phi, \eta_l, \eta_R; \nu_i^{(1)}, \nu_i^{(2)}, \nu_j^{(1)}, \nu_j^{(2)})$ so that

$$\frac{H}{k_B T} = \sum_{\langle ij \rangle} h_{4ij}^{(0)}(\phi, \eta_R, \eta_L; \nu_i^{(1)}, \nu_i^{(2)}, \nu_j^{(1)}, \nu_j^{(2)}) \ , \tag{4}$$

with $\phi = \theta_j^{(1)} - \theta_i^{(1)}$, $\eta_l = \theta_i^{(1)} - \theta_i^{(2)}$, $\eta_R = \theta_j^{(1)} - \theta_j^{(2)}$, the sum being again over nearest-neighbor sites on a hexagonal lattice. $h_{4ij}^{(n)}$, where n is the renormalization-group transformation index, is given initially by

$$\begin{aligned} h_{4ij}^{(0)}(\phi, \eta_L, \eta_R; \nu_i^{(1)}, \nu_i^{(2)}, \nu_j^{(1)}, \nu_j^{(2)}) &= \tilde{J}_1 \nu_i^{(1)} \nu_j^{(1)} V_{xy}(\phi) + \tilde{J}_2 \nu_i^{(2)} \nu_j^{(2)} V_{xy}(\phi + \eta_R - \eta_L) \\ &+ \frac{\tilde{J}_x}{Z}[\nu_i^{(1)} \nu_i^{(2)} V_{xy}(\eta_l) + \nu_j^{(1)} \nu_j^{(2)} V_{xy}(\eta_R)] + \tilde{K}_1(\nu_i^{(1)} - \nu_j^{(1)})^2 + \tilde{K}_2(\nu_i^{(2)} - \nu_j^{(2)})^2 \\ &+ \frac{\tilde{K}_x}{Z}[(\nu_i^{(1)} - \nu_i^{(2)})^2 + (\nu_j^{(1)} - \nu_j^{(2)})^2] - \frac{\tilde{\mu}_1}{Z}(\nu_i^{(1)} + \nu_j^{(1)}) - \frac{\tilde{\mu}_2}{Z}(\nu_i^{(2)} + \nu_j^{(2)}) \ . \end{aligned} \tag{5}$$

The cross bond linking the two lattices has been divided into $Z = 6$ equal parts, where Z is the number of nearest neighbors (within each layer) surrounding each site. A tilde over a coupling constant means that it has been divided by $k_B T$, e.g., $\tilde{J}_1 = J_1 / k_B T$.

Equation (5) has the simplicity of formally having reduced the two-layer system to an effective one-layer system with a "four-site" nearest-neighbor coupling. In the case where $J_x = K_x = 0$, the system decouples into two independent layers. The single-layer case has been studied by Berker and Nelson[1] for the triangular lattice and Cardy and Scalopino[2] for the square lattice.

The partition function for our system is now given by

$$Z = \prod_{i=1}^{N} \int_0^{2\pi} \frac{d\theta_i^{(1)}}{2\pi} \int_0^{2\pi} \frac{d\theta_i^{(2)}}{2\pi} \frac{1}{2} \sum_{\nu_i^{(1)}=0}^{1} \frac{1}{2} \sum_{\nu_i^{(2)}=0}^{1} e^{-H/k_B T} \ , \quad e^{-H/k_B T} = \prod_{\langle ij \rangle} U_{ij}^{(0)} \text{ and } U_{ij}^{(0)} = e^{-h_{4ij}^0} \ , \tag{6}$$

where N is the number of sites on a single lattice. We now invoke a Migdal-Kadanoff bond-moving transformation[9-11] in order to effect a systematic reduction of the degrees of freedom in Eq. (6). We may utilize the sheme of Berker and Nelson[1] as well as by us[8] in an earlier study of a two-layer ^{4}He system in the absence of ^{3}He impurities. We refer the reader to these articles for further details. Then we integrate and sum over the variables associated with the isolated sites. The recursion relation is easily found to be

$$\begin{aligned} &U^{(n+1)}(\theta, \eta_l, \eta_R; \nu_i^{(1)}, \nu_i^{(2)}, \nu_j^{(1)}, \nu_j^{(2)}) \\ &= \frac{1}{4} \sum_{t^{(1)}, t^{(2)}=0}^{1} \int_0^{2\pi} \frac{d\eta}{2\pi} \int_0^{2\pi} \frac{d\theta}{2\pi} \frac{[U^{(n)}(\phi, \eta_l, \eta; \nu_i^{(1)}, \nu_i^{(2)}, t^{(1)}, t^{(2)}) U^{(n)}(\theta - \phi, \eta, \eta_R; t^{(1)}, t^{(2)}, \nu_j^{(1)}, \nu_j^{(2)})]^2}{\frac{1}{4} \sum_{t^{(1)}, t^{(2)}=0}^{1} \int_0^{2\pi} \frac{d\eta}{2\pi} \int_0^{2\pi} \frac{d\phi}{2\pi} [U^{(n)}(\phi, 0, \eta; 0, 0, t^{(1)}, t^{(2)})]^4} \ , \end{aligned} \tag{7}$$

where we have used the reflection symmetry

$$U^{(n)}(\theta, \eta_L, \eta_R; \nu_i^{(1)}, \nu_i^{(2)}, \nu_j^{(1)}, \nu_j^{(2)}) = U^{(n)}(-\theta, \eta_R, \eta_L; \nu_j^{(1)}, \nu_j^{(2)}, \nu_i^{(1)}, \nu_i^{(2)})$$

and have chosen the normalization to ensure $U^{(n)}(0, 0, 0; 0, 0, 0, 0) = 1$. For convenience, we have dropped the subscripts ij on $U^{(n)}$ here and henceforth.

Note that Eq. (7) actually provides one with a set of 16 recursion relations since each of the occupation indices in Eq. (7) can assume two values. The reflection symmetry mentioned above reduces this number to 10, one of which is the normalization condition. $U^{(n)}$ does not in general factor into a sum of simple-pair and single-site terms as might be suggested by Eq. (5) and the definition (6) of $U^{(n)}$. Rather, $U^{(n)}$ must be thought of as a general four-site interaction. In order to extract useful information from iteration of Eq. (6), we write the general four-site Hamiltonian in the form

$$h_{4ij}^{(n)} = V_{xy}^{(n)}(\theta,\eta_R,\eta_L;\nu_i^{(1)},\nu_i^{(2)},\nu_j^{(1)},\nu_j^{(2)}) + \tilde{K}_1^{(n)}(\nu_i^{(1)}-\nu_j^{(1)})^2 + \tilde{K}_2^{(n)}(\nu_i^{(2)}-\nu_j^{(2)})^2$$
$$+\frac{\tilde{K}_x^{(n)}}{6}[(\nu_i^{(1)}-\nu_i^{(2)})^2+(\nu_j^{(1)}-\nu_j^{(2)})^2] + \tilde{K}_{22}^{(n)}(\nu_i^{(1)}\nu_j^{(2)}+\nu_i^{(2)}\nu_j^{(1)}) + \tilde{K}_{31}^{(n)}(\nu_i^{(1)}\nu_j^{(1)}\nu_j^{(2)}+\nu_j^{(1)}\nu_i^{(1)}\nu_i^{(2)})$$
$$+\tilde{K}_{32}^{(n)}(\nu_i^{(1)}\nu_i^{(2)}\nu_j^{(2)}+\nu_j^{(1)}\nu_i^{(2)}\nu_j^{(2)}) + \tilde{K}_4^{(n)}\nu_i^{(1)}\nu_i^{(2)}\nu_j^{(1)}\nu_j^{(2)} - \frac{\tilde{\mu}_1^{(n)}}{6}(\nu_i^{(1)}+\nu_j^{(1)}) - \frac{\tilde{\mu}_2^{(n)}}{6}(\nu_i^{(2)}+\nu_j^{(2)}) \ , \quad (8)$$

where

$$V_{xy}^{(n)}(0,0,0;0,0,0,0) \equiv 0 \ , \quad (9)$$

and $\tilde{K}_{22}$, $\tilde{K}_{31}$, $\tilde{K}_{32}$, $\tilde{K}_4$ are additional two-, three-, and four-site Ising interactions generated by the renormalization-group transformation. The general XY coupling potential $V_{xy}^{(n)}$ is assumed to obey reflection symmetry. The new Ising couplings have been chosen to obey this symmetry as well. At $\theta=\eta_R=\eta_L=0$, Eq. (7), with the normalization condition $U^{(n)}(0,0,0;0,0,0,0)=1$, provides nine recursion relations determining the seven Ising couplings and the two chemical potentials. Only five of these are of direct interest here. Expressions giving these are

$$\frac{\tilde{K}_x^{(n)}}{3} = -\ln U^{(n)}(000;1000) - \ln U^{(n)}(000;0100) + \ln U^{(n)}(000;1100) \ ,$$

$$\frac{\tilde{\mu}_1^{(n)}}{3} = \frac{\tilde{K}_x^{(n)}}{3} - \ln U^{(n)}(000;1010) \ ,$$

$$\frac{\tilde{\mu}_2^{(n)}}{2} = \frac{\tilde{K}_x^{(n)}}{3} - \ln U^{(n)}(000;0101) \ , \quad (10)$$

$$\tilde{K}_1^{(n)} = -\ln U^{(n)}(000;1000) + \tfrac{1}{2}\ln U^{(n)}(000;1010) \ ,$$

$$\tilde{K}_2^{(n)} = -\ln U^{(n)}(000;0010) + \tfrac{1}{2}\ln U^{(n)}(000;0101) \ .$$

We find that in all situations $K_x^{(n)}$ iterates to infinity. The behavior of the other four parameters in Eq. (10) is much more interesting in that it reflects closely the nature of the first-order transitions found in our model. The effective XY coupling for our system is calculated from a procedure motivated by our earlier work[7] on a two-layer model for pure ^{4}He. In that work, the XY cross coupling always iterated to infinity. This phenomenon occurs in the present, more complicated, model as well. Explicitly, this means that the function $V_{xy}^{(n)}(\theta,\eta_R,\eta_L,1111)$ becomes very sharply peaked in η_R and η_L and a Villain form in θ for large n, i.e.,

$$\frac{U^{(n)}(\theta,\eta_L,\eta_L;1111)}{U^{(n)}(0,0,0;1111)} \to \tilde{\delta}(\eta_l)\tilde{\delta}(\eta_R)e^{h_2(\theta)} \ , \quad (11)$$

where $h_2(\theta)$ can be described by a Villain[12] form

$$h_2(\theta) = \sum_{m=-\infty}^{\infty} e^{-\tilde{J}_v(\theta-2\pi m)^2/2} \Big/ \sum_{m=-\infty}^{\infty} e^{-\tilde{J}_v(2\pi m)^2/2} \ . \quad (12)$$

In Eq. (11) $\tilde{\delta}(\eta)$ is a very sharply peaked function at $\eta=0$. We monitor the behavior of the XY couplings by defining the effective temperatures

$$(T_{xy}^{(n)})^{-1} = -\ln\left[\frac{U^{(n)}(\pi,0,0;1111)}{U^{(n)}(0,0,0;1111)}\right] \ , \quad (13)$$

$$(T_x^{(n)})^{-1} = -\ln\left[\frac{U^{(n)}(0,\pi\pi;1111)}{U^{(n)}(000;1111)}\right] \ . \quad (14)$$

Note that $T_{xy}^{(n)}$, which measures the total two-layer XY coupling is initially given by $T_{xy}^{(0)}=\frac{1}{2}(\tilde{J}_1+\tilde{J}_2)^{-1}$, whereas the measure of the XY cross-coupling $T_x^{(n)}$ is initially given by $T_x^{(n)}=3/2\tilde{J}_x$. $T_x^{(n)}$ always iterates rapidly toward low temperatures for all cases considered. This fact is responsible for the behavior shown in Eq. (11). This same phenomenon occurs in a two-layer model for pure ^{4}He.[8]

$T_{xy}^{(n)}$ may be simply related to the Villain coupling $\tilde{J}_v$ [neglecting negligible contributions from terms with $|m|>1$ in Eq. (12)] by

$$T_{xy}^{(n)} \underset{n>>1}{\to} \left[\frac{\tilde{J}_v}{2}\pi^2 - \ln 2\right]^{-1} \ , \quad (15)$$

when $\tilde{J}_v \neq 0$ and $\tilde{J}_v=0$ when $T_{xy}^{(n)} \to \infty$.

For pure ^{4}He (Ref. 8) we derived the approximate relation

$$\frac{\sigma_s(T)}{k_B T} \approx \left(\frac{m^2}{\hbar^2}\right)\tilde{J}_v \ . \quad (16)$$

This holds in the present case as well. For $T=0$ it is

easy to see that

$$\sigma_s(0) = m^2 k_B (J_1 + J_2)/\hbar^2 \ .$$

A convenient relation then derived from Eq. (15) and Eq. (16) is

$$\frac{\sigma_s(T)}{\sigma_s(0)} \cong \frac{2}{\pi^2} \frac{[(T_{xy}^f)^{-1} + \ln 2]}{J_1 + J_2} \ , \tag{17}$$

where T_{xy}^f is the approximately determined fixed-point value of $T_{xy}^{(n)}$. The determination of T_{xy}^f is discussed in detail in Sec. IV.

To obtain the ^{3}He concentrations $X_3^{(1)}$ and $X_3^{(2)}$ in the two layers, we utilize the identities

$$\begin{aligned} -\frac{\partial F}{\partial \tilde{\mu}_1} &= \langle \nu_i^{(1)} \rangle = 1 - X_3^{(1)} \ , \\ -\frac{\partial F}{\partial \tilde{\mu}_2} &= \langle \nu_i^{(2)} \rangle = 1 - X_3^{(2)} \ , \end{aligned} \tag{18}$$

where F is the free energy obtained via the method of Nauenberg and Nienhuis.[13] Explicitly,

$$F = \tfrac{3}{4} \sum_{n=0}^{\infty} \frac{g_n}{4^n} \ , \tag{19}$$

in which g_n is the normalization constant of the renormalization-group transformation, i.e., the denominator of Eq. (7).

III. DESCRIPTION OF RESULTS

In this section we provide a description of our results, deferring a discussion of the details of how they were derived to the following section.

As mentioned in Sec. I (see also Sec. V), we present results obtained from the renormalization transformation (7) for the case $K_1 = K_2 = K_x = J_1 = J_2 = 1.0$ (in units of k_B) and $J_x = 0.05$.

It is useful to begin with a description of phase diagrams in the $\mu_1 - \mu_2$ plane at fixed T. For $T = 0$, this diagram may be determined analytically. The result is shown in Fig. 1. Because there is symmetry about the line $\mu_1 = \mu_2$, we only show that case $\mu_2 \geq \mu_1$. The diagram is divided into three separate regions, or phases:

a. Phase 3-3. In this phase both layers are pure ^{3}He and the system is normal (i.e., nonsuperfluid).

b. Phase 3-4. In this phase layer 2 is pure ^{4}He and layer 1 is pure ^{3}He. This phase is superfluid.

c. Phase 4-4. In this phase both layers are pure ^{4}He and the sytem is superfluid.

The line AB separating regions 3-3 and 3-4 is a first-order line for phase separation in layer 2. BC is a first-order line for phase separation in layer 1. BD is a first-order line for phase separation in both layers simultaneously. The point B is a three-phase coexistence point.

The situation at $T = 1.0$ is depicted in Fig. 2. This

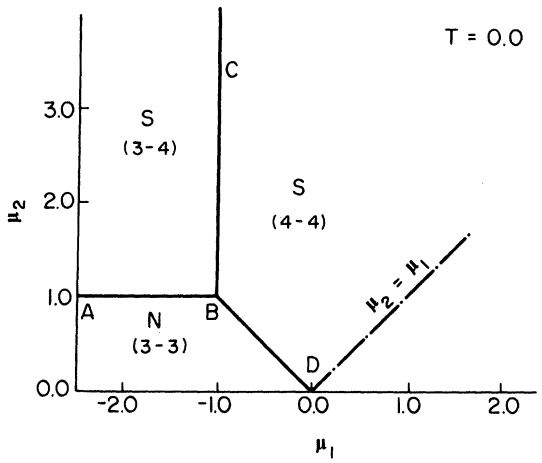

FIG. 1. Phase diagram for $T = 0$, in the $\mu_1 - \mu_2$ plane. 3-3, 3-4, and 4-4 are the three phases corresponding to layer 1 and layer 2 being ^{3}He rich-^{3}He rich, ^{3}He rich-^{4}He rich, and ^{4}He rich-^{4}He rich, respectively. The coupling is $K_1 = K_2 = K_x = J_1 = J_2 = 1.0$ and $J_x = 0.05$ (in units of k_B). N and S indicate normal and superfluid phases, respectively.

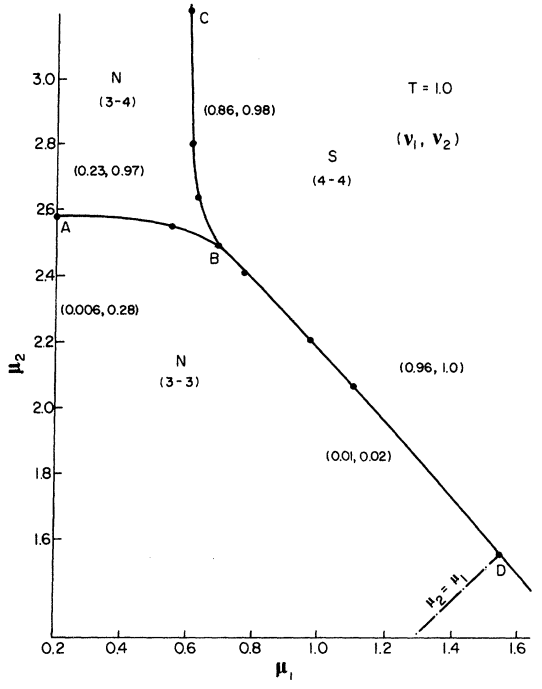

FIG. 2. Phase diagram for $T = 1.0$, in the $\mu_1 - \mu_2$ plane. 3-3, 3-4, and 4-4 are the three phases corresponding to layer 1 and layer 2 being ^{3}He rich-^{3}He rich, ^{3}He rich-^{4}He rich, and ^{4}He rich-^{4}He rich, respectively. The coupling is $K_1 = K_2 = K_x = J_1 = J_2 = 1.0$ and $J_x = 0.05$ (in units of k_B). N and S indicate normal and superfluid phases, respectively. Some representative concentrations for ^{4}He are given as (ν_1, ν_2) for layers 1 and 2, respectively. The dots on the lines show the computed points.

diagram is quite similar to that at $T=0$. The differences are that the three-phase coexistence point has been displaced, phase 3-4 is no longer superfluid, and the phases are no longer pure, e.g., in 3-3 both phases are ^{3}He rich but contain some ^{4}He. Further, the transition across AB involves discontinuities in both $X_3^{(1)}$ and $X_3^{(2)}$, the major discontinuity being in $X_3^{(2)}$. The situation is reversed across BC. In Fig. 2 some representative ^{4}He concentrations for the two layers are given as (ν_1, ν_2).

At $T=1.30$ the results are shown in Fig. 3. Here there is a new feature. The onset of superfluidity which was first order and occurred along the line CBD at $T=1.0$ is now second order and occurs along the λ line SO. A similar phenomenon also occurs at about $T=0.94$. Here the line AB which involves a first-order transition to a superfluid phase at $T=0$ no longer involves superfluidity. Rather, there is a λ line across the region bounded by AB and BC. This line merges with the first-order superfluid line BC at $T\cong 0.95$. The resulting line remains first order for superfluidity until $T\approx 1.25$ where the λ line SO in Fig. 3 departs from BC toward the right. We find that the jump in $\sigma_s(T)/T$ across SO is universal, as expected.[8,14]

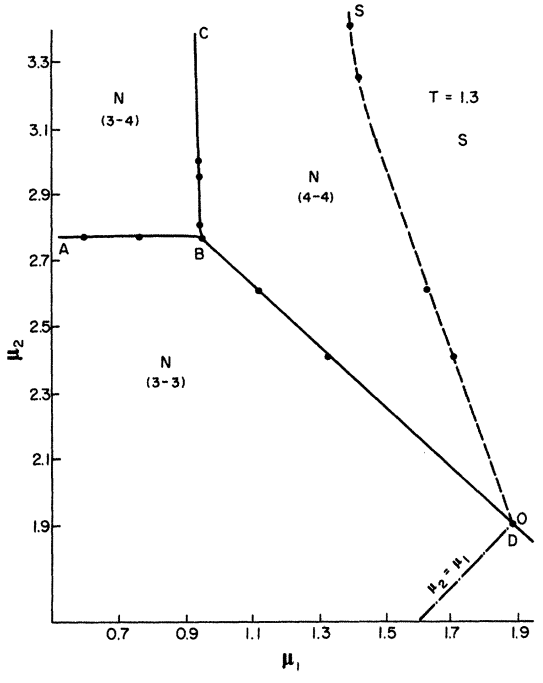

FIG. 3. Phase diagram for $T=1.3$, in the $\mu_1-\mu_2$ plane. 3-3, 3-4, and 4-4 are the three phases corresponding to layer 1 and layer 2 being ^{3}He rich-^{3}He rich, ^{3}He rich-^{4}He, and ^{4}He rich-^{4}He rich, respectively. The coupling is $K_1=K_2=K_x=J_1=J_2=1.0$ and $J_x=0.05$ (in units of k_B). N and S indicate normal and superfluid phases, respectively.

At $T=1.38$ (the λ temperature for the pure ^{4}He system[8]) the λ line SO of Fig. 3 has receded to infinity, and all phases are normal. The first-order lines for phase separation disappear at higher temperatures and they appear to do so in the following rather interesting way. As T is increased, the ends of lines AB and BC, which at low T are at infinity, recede from infinity toward the point B of three-phase coexistence. In this case the points B and C are critical points corresponding to consolute points. At higher T the lines AB and BC vanish altogether, B ceases to be a three-phase coexistence point and BD shrinks until only D remains at the critical consolute temperature for $\Delta\mu=0$. For higher T there are no phase transitions. Our evidence for this sequence is not, however, complete. It is based on our analytic result at $T=0$ and the locations of consolute temperatures for the cases $\Delta\mu=2.0$, 1.8, and 0.0 discussed below.

A given physical system has a fixed difference $\Delta\mu=\mu_2-\mu_1$ imposed by the presence of the substrate and the discrete nature of the ^{3}He energy levels (see the Introduction). An experiment can vary μ_1 at fixed $\Delta\mu$ and T, taking the system along a line parallel to the 45° line $\mu_1=\mu_2$ in Figs. 1–3. We therefore calculate phase diagrams at constant $\Delta\mu$. Several cases are treated.

1. $\Delta\mu=2.0$

This is the case where three-phase coexistence occurs at $T=0$. In Fig. 4 we show the μ_1-T diagram. One easily can see the relation of Fig. 4 to Figs. 1–3. For example, in Fig. 2 for $T=1.30$ moving along the line $\Delta\mu=2.0$ one passes successively through the first-order lines AB and BC and finally through the λ line SO. This sequence is repeated moving horizon-

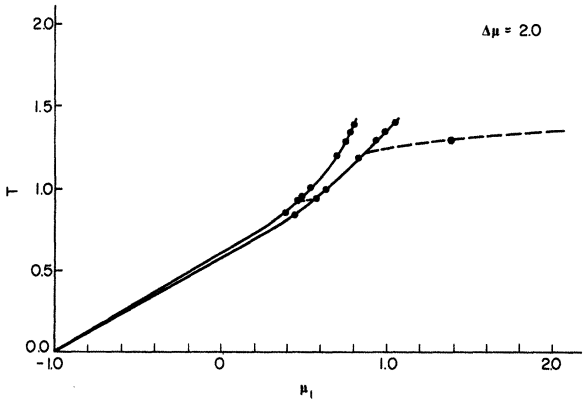

FIG. 4. Phase diagram for $\Delta\mu=2.0$ in the $T-\mu_1$ plane. Solid lines are first-order transitions and dashed lines are the superfluid transitions. The couplings are same as Fig. 1. The dots indicate computed points.

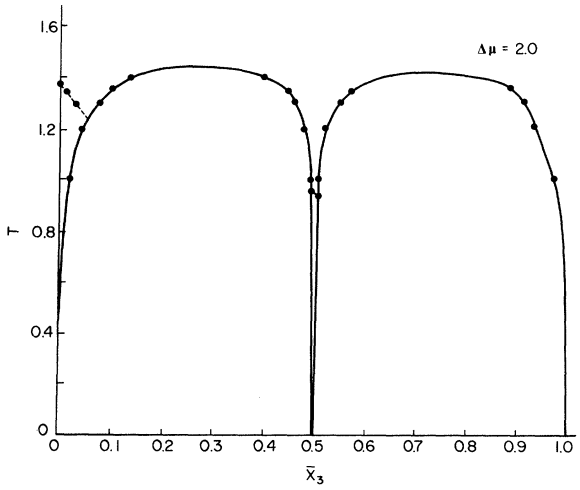

FIG. 5. Phase diagram for $\Delta\mu = 2.0$ in the $T - \bar{X}_3$ plane. There are two λ lines, one indicated by dashed lines and the other (between the two lobes) by a short solid line. Dots indicate computed points. The couplings are the same as in Fig. 1.

tally from left to right at $T = 1.30$ in Fig. 4.

It is useful to define the average ^{3}He concentration $\bar{X}_3$ by

$$\bar{X}_3 = \frac{X_3^{(1)} + X_3^{(2)}}{2} \quad . \tag{20}$$

Then we can construct the $\bar{X}_3 - T$ diagram corresponding to Fig. 4. The result is shown in Fig. 5, where the right-hand coexistence region corresponds to the left-hand first order of Fig. 4. Note that for $T \leq 0.95$ it is possible to have two coexisting superfluid phases.

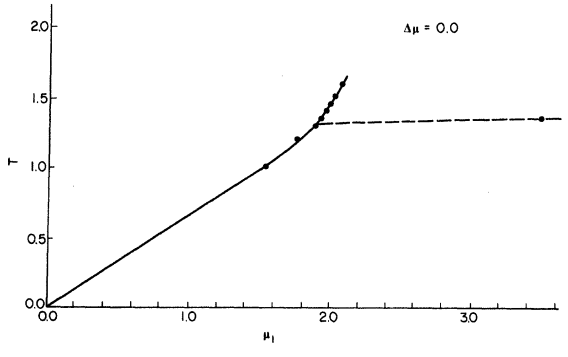

FIG. 6. Phase diagram for $\Delta\mu = 0$ in the $T - \mu_1$ plane. Solid lines are first-order transitions and the dashed line is the λ line. The couplings are same as Fig. 1. The dots indicate computed points.

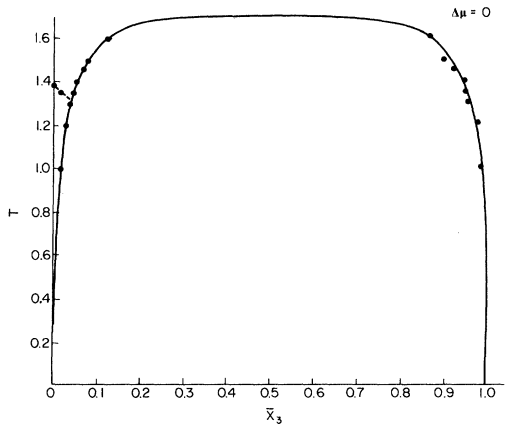

FIG. 7. Phase diagram for $\Delta\mu = 0$ in the $T - \bar{X}_3$ plane. The single λ line is shown as a dashed line. Dots indicate computed points. The couplings are the same as in Fig. 1.

2. $\Delta\mu = 0$

For this situation there is no three-phase coexistence, as one sees upon looking once again at Figs. 1–3. The two layers are identical, there being no difference between μ_1 and μ_2 to produce the two first-order transitions appearing in the case $\Delta\mu = 2.0$.

The phase diagrams in the $\mu_1 - T$ and $\bar{X}_3 - T$ planes are given in Figs. 6 and 7.

3. $\Delta\mu = 1.8$

This value of $\Delta\mu$ is chosen in order to exhibit a situation in which the three-phase coexistence occurs at nonzero T. In Fig. 8 we show the $\mu_1 - T$ diagram. Below $T \cong 1.3$ there is only a single first-order transition. Above $T \cong 1.3$ there are two first-order transitions as indicated by the fork in the solid line. The apex of the fork is a point of three-phase coexistence.

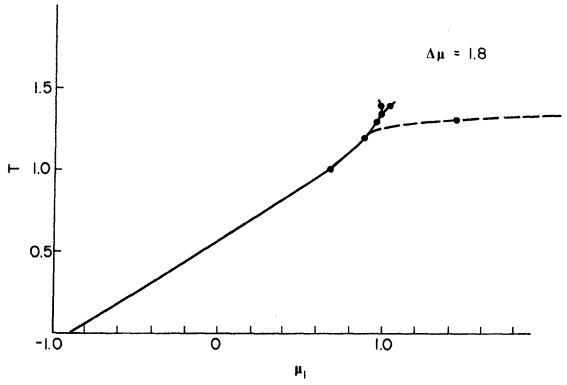

FIG. 8. Phase diagram for $\Delta\mu = 1.8$ in the $T - \mu_1$ plane. Solid lines are first-order transitions and the dashed line is the λ line. The couplings are same as Fig. 1. The dots indicate computed points.

There is a single λ line occurring for this case. A slight increase in $\Delta\mu$ would bring the tip of the λ line in coincidence with the apex. This is a case where three first-order lines and a λ line terminate at the same point, and where three-phase coexistence occurs in which one phase is superfluid and two are normal.

Figure 9 shows the $\bar{X}_3 - T$ diagram for $\Delta\mu = 1.8$. Given the results summarized in Figs. 1–9, it is possible to speculate on what variation of the fixed parameters K_1, K_2, K_x, J_1, J_2, and J_x would produce. In our work on the pure ^{4}He case increasing J_x merely raised the λ temperature. In the present case increasing J_x is then expected to raise the λ lines in the $\bar{X}_3 - T$ figures. Setting the Ising couplings in Eq. (1) equal to zero so that $K_i = J_i/2$ $(i = 1, 2, x)$ in Eq. (3) is expected to move the left-hand λ line in our $\bar{X}_3 - T$ figures near to the top of the left-hand phase-separation curves, as this occurs in the BNCS[1,2] one-layer models. Making $K_1 << K_2$ could produce very interesting behavior. We speculate that this would make the tip of the left-hand phase-separation curve drop to lower temperatures so that the two λ lines would merge into a single line passing above the left-hand coexistence region and hitting the right-hand coexistence region on its left side. This would produce the phenomenon of critical phase separation between two superfluid phases.

Phenomena similar to the two transitions seen in Fig. 5 have been observed in lattice-gas models[15,16] for adsorption of classical gases onto substrates. In these situations it is possible to have an infinite number of transitions, one corresponding to each added layer of adsorbed film. It is also possible to have transitions corresponding to several layers at once, a feature found in our model (see, e.g., Fig. 7). Further, the dependence of consolute temperatures

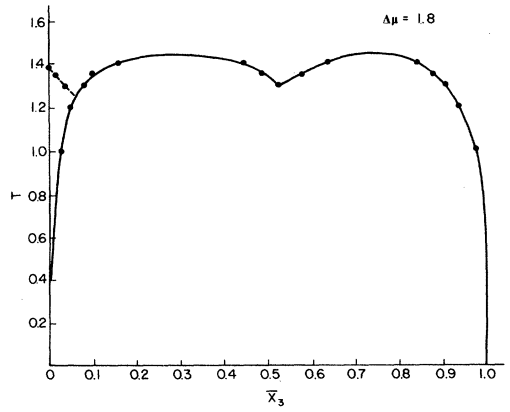

FIG. 9. Phase diagram for $\Delta\mu = 1.8$ in the $T - \bar{X}_3$ plane. The single λ line is shown as a dashed line. Dots indicate computed points. The couplings are the same as in Fig. 1.

on the substrate field ($\Delta\mu$ in our case) in the adsorption models[16] is similar to what we find.

This concludes our description of the phase diagrams obtained from Eq. (7). We remark that our results are based on an approximate renormalization-group scheme. However, we feel that the qualitative features of these results are correct. In the following section we provide some detail concerning how the diagrams were found. A discussion of the superfluid density is deferred to Sec. V where we discuss our results in comparison with experiment.

IV. CALCULATIONAL DETAILS

The $T = 0$ phase diagrams are easily obtained by finding the ground state of H in Eq. (3). For $T \neq 0$ our results follow from implementation of the Migdal-Kadanoff recursion relation, Eq. (7). The integrals were performed numerically using a double Simpson-rule method, the calculations being done in real space as opposed to Fourier space because of the difficulty of representing the sharply peaked function $\tilde{\delta}(\eta)$ [see Eq. (11)] as a Fourier sum.

To determine whether or not a given phase is superfluid we have examined the behavior of $T_{xy}^{(n)}$ [see Eqs. (13) and (17)] under iteration of Eq. (7). The analysis is identical to that of Ref. 8. Superfluid onset at λ lines was found to be universal as expected. This universality does not, of course, apply to a first-order transition to a superfluid state, where $\sigma_s(T)/T$ jumps from zero to a value larger than the universal one[8,14] applicable at a λ line.

The first-order transitions in our model are dominated by the Ising couplings and chemical potentials appearing in Eq. (3). How these behave under iteration is simply understood by looking at the one-layer problem in the absence of XY coupling. The recursion relations for the Ising coupling K_n and the chemical potential μ_n are in this case easily obtained analytically. One finds a first-order line at $\mu = 0$ and $K = \infty$, terminated at a critical fixed point $\mu_c^* = 0$, $K_c^* = 0.6094$. Away from the first-order line K_n always iterates to zero, while μ_n iterates to plus (minus) infinity for positive (negative) initial values μ_0. This behavior occurs in each layer the full two-layer model of Eq. (3), and allowed a quick approximate location of the first-order transitions, which were then closely pinpointed by examining both the behaviors of Ising couplings and chemical potentials and of the ^{3}He concentrations calculated from Eq. (18).

In all cases considered, the variables $J_x^{(n)} \sim 1/T_x^{(n)}$ and $K_x^{(n)}$ iterate rapidly toward infinity; they are thus always irrelevant variables. For completeness, we show in Fig. 10 the computed average concentration $\bar{X}_3$ for $T = 1.3$ and $\Delta\mu = 2.0$ as a function of μ_1. The observed discontinuities are, moving from left to

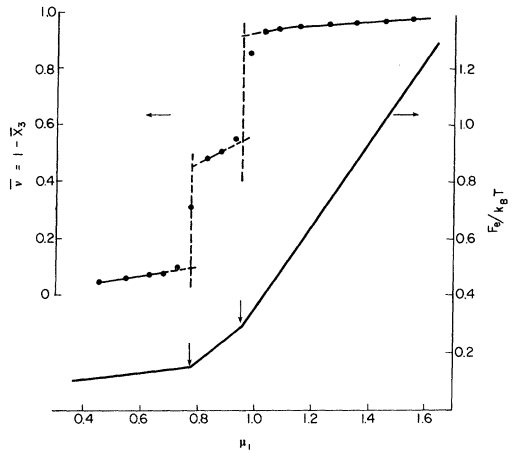

FIG. 10. Free energy is plotted vs μ_2 for $T=1.3$ and $\Delta\mu=2.0$ on the right. On the left is the averaged concentration of ^{4}He for the two-layer system as a function of μ_1. The coupling is the same as for Fig. 1. Dots indicate computed points. Vertical arrows locate the phase-separation transitions. Dashed lines show extrapolations.

right, those occurring in Fig. 2 as one moves along the diagonal line $\Delta\mu=2.0$ across AB and then across BC. Note that the discontinuities are not perfectly sharp, primarily as a consequence of not using an infinitely fine grid in μ_1. The actual value of μ_1 at the transition has been determined from a plot of the free energy F (inset in Fig. 10). The point of discontinuity in the slope of F, determined by extrapolation (see Fig. 10) from the left and right, has been used to find μ_1 at the transition. The concentrations in the two phases at the transition value of μ_1 are determined by extrapolation to this value of μ_1 from the left and right of the $\bar{X}_3$ diagram. These extrapolations are also indicated in Fig. 10.

In the following section we relate our results to experiment, showing in detail a plot of σ_s indicating two superfluid transitions.

V. RELATION TO EXPERIMENT

As mentioned in the Introduction, the BNCS theory for a one-layer ^{3}He-^{4}He mixture film is incapable of producing the two superfluid transitions observed by Bishop and Reppy.[7] Our two-layer model has considerably more flexibility and can, in fact, produce transitions qualitatively similar to those of

from zero with decreasing T as more and more of the superfluid phase is created at the expense of the normal phase. Finally, the normal phase will cross the λ line connecting the consolute curves and suddenly become superfluid causing a large jump in σ_s for the whole system. A plot of $\sigma_s(T)/\sigma_s(0)$ [see Eq. (17)] for this situation is given in Fig. 11. Note that the value $\Delta\mu=2.0k_B$ for Fig. 5 is consistent with our estimate $\Delta\mu\sim k_B$ given in Sec. I.

It is expected that a value of J_x considerably larger than 0.05, e.g., $J_x=1.0$ could cause the two λ lines in Fig. 5 to occur at such high temperatures that they would join above the left-hand consolute point, thus eliminating the two-transition nature of the result. An extrapolation of the pure ^{4}He results[7] suggests that this would happen, the λ temperatures rising about 60%. However, if when J_x were increased, the Ising couplings were also increased by 60%, the consolute temperatures would rise by about the same amount, and the two-transition character would remain. Such an increase in Ising couplings is consistent with our order-of-magnitude estimates for the couplings given in Sec. I. It thus seems likely that there will be a range of parameters for which the two transitions will occur. We were unable to investigate this point; in fact, treating the case $J_x=1.0$ was not computationally feasible.[17]

It must be pointed out that the experiment reported by Bishop and Reppy[6] was done with a ^{4}He film having approximately one active layer to which was added 10 at.% ^{3}He. At $\bar{X}_2=10\%$ in Fig. 5 it is clear that decreasing T would produce two discontinuous jumps in $\sigma_s(T)$ in contrast to the behavior viewed in Fig. 11. The two-layer model which we have presented thus does not quantitatively reproduce the experimental observations. There is, qualitative agreement with experiment, as illustrated in Figs. 5 and 11. This qualitative agreement is a consequence of our inclusion of the known discrete nature of ^{3}He levels in thin ^{4}He films. This discreteness should perhaps

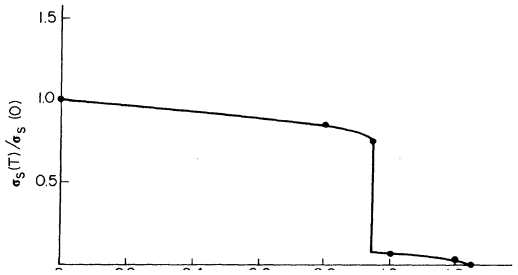

be an essential feature of any better model of the Bishop-Reppy experiment. A possible improved model would be a two-layer model with ^{4}He's and two types of impurities, ^{3}He's and vacancies. We have not attempted to deal with this more complicated situation, but we anticipate that it would produce behavior similar to but even more rich than the model treated in this work.

We remark finally that there exist other experiments[18,19] on ^{3}He-^{4}He mixture films which do not appear to show two superfluid transitions. These experiments, however, were done at higher temperatures with thicker films where the discreteness of ^{3}He levels might cease to be a factor. These experiments also showed solubilities of up to 40 at.% for ^{3}He in ^{4}He in the superfluid phase of the films. The BNCS[1,2] theories limit this solubility to about 20 at.%. The present work allows single-phase superfluidity up to concentrations of ~50 at.%, as is seen in Fig. 5. We encourage further experimentation.

ACKNOWLEDGMENTS

We wish to thank Dr. David Bishop and Dr. Frank Gasparini for conversations about their experiments. This work was supported in part by the National Science Foundation under Grant No. DMR-7906934.

---

*Present address: Coordinated Science Laboratory, University of Illinois at Urbana-Champaign, Urbana, Ill. 618801.

[1]A. N. Berker and D. R. Nelson, Phys. Rev. B 19, 2488 (1979).

[2]J. L. Cardy and D. J. Scalapino, Phys. Rev. B 19, 1428 (1979).

[3]J. P. Laheurte, J. P. Romagnan, and W. F. Saam, Phys. Rev. B 15, 4214 (1977).

[4]W. F. Saam, Phys. Rev. A 4, 1278 (1971).

[5]M. J. DiPirro and F. M. Gasparini, Phys. Rev. Lett. 44, 269 (1980).

[6]G. Baym, Phys. Rev. Lett. 18, 71 (1967).

[7]D. J. Bishop and J. D. Reppy, Phys. Rev. B 22, 5171 (1980).

[8]K. K. Mon and W. F. Saam, Phys. Rev. B 22, 3221 (1980).

[9]A. A. Migdal, Zh. Eksp. Teor. Fiz. 69, 1457 (1975) [Sov. Phys. JETP 42, 743 (1976)].

[10]J. V. José, L. P. Kadanoff, S. Kirkpatrick, and D. R. Nelson, Phys. Rev. B 16, 1217 (1977).

[11]L. P. Kadanoff, Ann. Phys. (N.Y.) 100, 359 (1976).

[12]J. Villain, J. Phys. (Paris) 36, 581 (1975).

[13]M. Nauenberg and B. Nienhuis, Phys. Rev. Lett. 33, 1598 (1974).

[14]D. R. Nelson and J. M. Kosterlitz, Phys. Rev. Lett. 40, 1454 (1978).

[15]M. J. de Oliveira and R. B. Griffiths, Surf. Sci. 71, 689 (1978).

[16]C. Ebner has performed both mean-field [Phys. Rev. A 22, 2776 (1980)] and Monte Carlo calculations [Phys. Rev. A (in press)] for several substrate potential strengths.

[17]For J_x much larger than 0.05 the function $V_{xy}^{(n)}(\theta, \eta_R, \eta_I; 1111)$ [see Eqs. (8) and (11)] became too sharply peaked too rapidly to handle with a computationally reasonable integration net, given the large number of double-integral recursion relations in Eq. (7). Computer time on an Amdahl 470/168 required to obtain points at a single temperature for Fig. 5 was in excess of one hour. Working with $J_x = 1.0$ would require doubling our net size with a consequent increase in computer time by more than an order of magnitude.

[18]E. Webster, G. Webster, and M. Chester, Phys. Rev. Lett. 42, 243 (1979).

[19]J. P. Laheurte, J. C. Noiray, and J. P. Romagnan, Phys. Rev. B 22, 4307 (1980).